Chapter 10
Micro pH Sensors and Biosensors Based on Electrochemical Field Effect Transistors

Junji Sasano, Daisuke Niwa, and Tetsuya Osaka

10.1 Fabrication of On-Chip FET pH Sensor

10.1.1 Introduction

A study on ion-sensing using field effect transistor (FET) was begun by Bergveld in the 1970s [1–3]. The ion-sensitive (IS) FET is now widely used as a miniaturized pH sensor, commercialized by some companies. First, the principle and structure of the ISFET are introduced in this section. A basic design of ISFET is shown in Fig. 10.1a. ISFET has silicon substrate with field-effect structures such as electrolyte/IS layer/(insulator)/semiconductor structures; the space charge region in the semiconductor is modulated depending on the gate voltage (V_g), same as a typical metal-oxide-semiconductor (MOS) FET. A typical bias V_g versus drain-source current (I_{ds}) characteristic of the device that has silicon nitride/silicon dioxide/silicon is shown in Fig. 10.1b. This characteristic is quite similar to the MOSFET. A prominent difference between ISFET and MOSFET is that the gate voltage for the operation of the device is applied by an electrochemical reference electrode through the electrolyte in contact with the gate insulator. The threshold voltage (V_{th}) could shift according to the value of the pH of the solution. In the MOSFET, the V_{th} would shift

J. Sasano
Consolidated Research Institute for Advanced Science and Medical Care, Waseda University, 513 Wasedatsurumaki-cho, Shinjuku-ku, Tokyo 162-0041, Japan; Department of Production Systems Engineering, Toyohashi University of Technology

D. Niwa
Consolidated Research Institute for Advanced Science and Medical Care, Waseda University, 513 Wasedatsurumaki-cho, Shinjuku-ku, Tokyo 162-0041, Japan; Nano Bionics R&D Center, ROHM Co., Ltd.

T. Osaka (✉)
Consolidated Research Institute for Advanced Science and Medical Care, Waseda University, 513 Wasedatsurumaki-cho, Shinjuku-ku, Tokyo 162-0041, Japan; School of Science and Engineering, Waseda University, 3-4-1 Okubo, Shinjuku-ku, Tokyo 169-8555, Japan
e-mail: osakatets@waseda.jp

T. Osaka et al. (eds.), *Electrochemical Nanotechnologies,*
Nanostructure Science and Technology, DOI 10.1007/978-1-4419-1424-8_10,

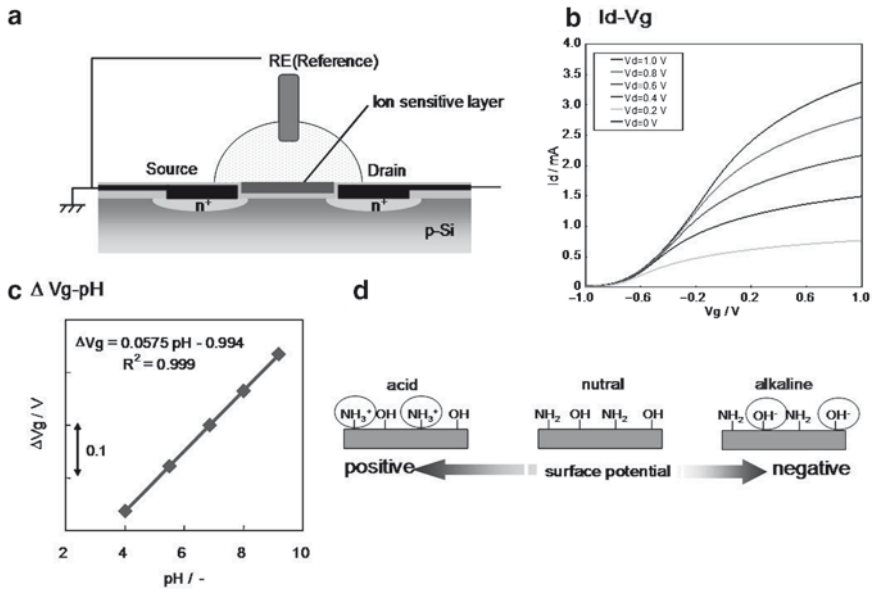

Fig. 10.1 (**a**) Basic design of ISFET. (**b**) I_{ds}–V_g characteristics of the device. (**c**) pH responsibility of the device. (**d**) Change in the surface structure and surface potential of silicon nitride layer in each pH solution

depending on the change in the space charge region in the MOS capacitor structure by the application of V_g. On the other hand, the V_{th} in ISFET would shift according to the change in the surface potential in the electrolyte/IS layer interface. Therefore, the IS layers and their interfaces in ISFET play an important role in the performance of pH responsibility. It is well-known that the silicon nitride surface shows a good pH response in solution. The silicon nitride layer is often formed by plasma-enhanced chemical vapor deposition (PECVD), which is generally formed at the thickness of 100–500 nm. The V_g vs. $I_{ds,}$ characteristics of the silicon nitride-based ISFET indicate a good pH responsibility of 58 mV/decade that shows Nernstian response (Fig. 10.1c). The shift of the V_{th} depends on the changes of surface potential at electrolyte/silicon nitride interface. On the silicon nitride surface immersed in aqueous solution, both amphoteric Si–OH sites and basic Si–NH_2 sites (Fig. 10.1d) are produced by hydrolysis. These sites directly interact with the solution to either bind or release hydrogen ions, leading to bear a certain surface charge on the nitride surface that was opposed to an ionic charge in the solution. This formed a double-layer capacitance across which the potential drop occurs. Therefore, the threshold voltage shifted accompanied by the pH change in solution.

Based on this principle, ISFET is used gradually for the detector as various sensing materials. However, since 1990s, such active research has declined due to various problems, such as the stability of the device and the molecular modification on the electrode surface. On the other hand, the research of FET has begun to steal the limelight again by the progress of the technologies of the semiconductor device fabrication and the surface modification. Especially, the development of IS layers

and new device processing has been studied for the improvement of the performance of ISFET itself. Currently, Ta_2O_5 [4] is often used as an insulating layer. However, to construct the high-performance FET sensor, it should be necessary to improve the device architecture.

In this section, new type FET-based sensors are described focusing mainly on the research activities in nanotechnology at Waseda University.

10.1.2 Concept of On-chip pH Sensors Using FETs Modified with Self-Assembled Monolayers

The aim of our study is to fabricate an extremely high-performance ion and biosensing device. In our work, we have studied the fabrication of FET-based ion and biosensor using self-assembled monolayers (SAMs) [5–9]. Our concept and details of device architecture are described in the following lines.

In order to realize highly sensitive biosensing system, *precise fabrication* of the electrode parts for molecular recognition is a significant issue. For this purpose, development of new detection devices with high sensitivity is strongly demanded. It is especially desired that the electrode surfaces have the supramolecular structure that mimics cell systems. In order to fabricate such an electrode, application of the template for the ordered-arrangement of the molecules is effective. Organic monolayers have the ability to self-assemble onto the surfaces [10, 11]; the monolayer-modified electrode is suitable as the template for orderly immobilization of biomolecules. On the other hand, it is preferable that the detection system can detect the signal immediately and very sensitively. A FET type electrode can detect the response of surface reactions as an electric signal, with capability for on-chip integration. Therefore, we have studied the formation of electrodes functionalized by the modification of organic monolayer on silicon wafer surfaces and the development of the detection system utilizing a semiconductor device such as a FET.

Figure 10.2 shows the basic design of the on-chip integrated biosensing devices including reference devices. For the on-chip sensing, reference device as well as sensing device is necessary. In general, a glass-based Ag/AgCl electrode is used as a reference electrode. However, the glass electrode is hard to miniaturize and is easy to break. The use of such a glass electrode acts as a high barrier in the miniaturization of the sensor chip. Therefore, the development of a small and solid-based reference electrode is desired for the realization of the on-chip sensors. Utilizing the functionality of an organic monolayer is expected to be one of the solutions to the problem. In order to fabricate the sensor and the reference devices, it is required that the organic monolayers having different functional groups are area-selectively immobilized on each gate electrode. At the sensing electrode, amino-functionalized monolayer, which is an active site, is suitable for immobilization of biomaterials, enzyme, etc. as well as ion response. For the reference electrode, an alkyl, or perfluoro-alkyl functionalized monolayer having inactive functional group is effective for preventing any undesired adsorptions and ionic reactions at the surface. Hence,

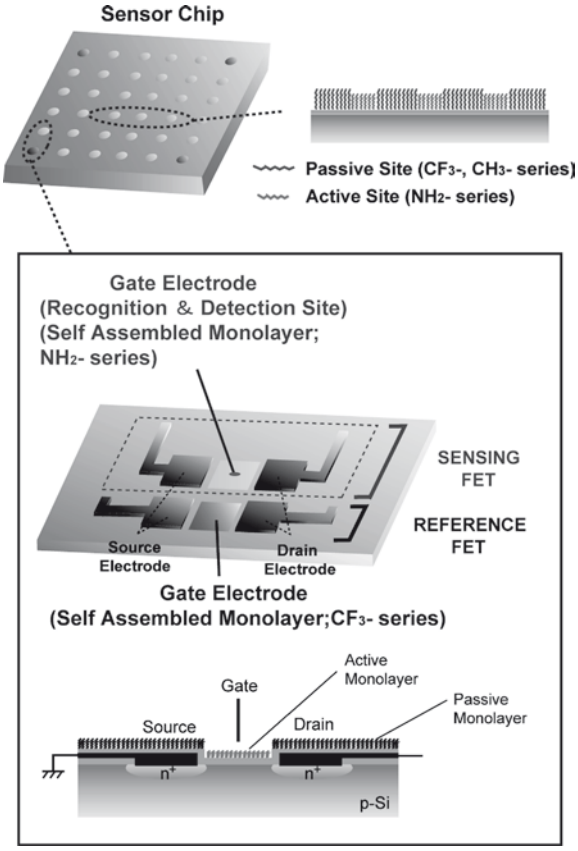

Fig. 10.2 Schematic design of on-chip FET sensing device

the formation of various functionalized monolayers and their patterning are one of the *key* processes for fabricating on-chip biosensing devices.

It is assumed that such an on-chip sensing device has the ability accurately detect the single molecule. Especially, formation of very thin monolayer on the electrode enables immediate detection of the signal that originates in the bioreaction. Moreover, it seems that effective arrangements of molecules, during the bioreaction, onto the electrodes are acquired by using the monolayer templates. The multi-detection of the molecule is expected to be achieved because this device is easy to miniaturize and integrate. On the other hand, FETs are required to have a high chemical durability because they are exposed to various types of solutions during the sensing, the surface cleaning, and the molecular modification processes.

In our work, we have investigated the fabrication of the FET devices with various functionalized SiO_2-gate modified with organosilane monolayers. The pH sensitivity and chemical durability of the devices are evaluated as the basic characteristic of the devices.

10.1.3 Formation of Organosilane Monolayer on Silicon Surface

Organosilane SAMs have been widely applied to control physical and chemical properties of the surfaces of glass, quartz, SiO_2/Si wafer, and silica particle [10]. Many researchers have studied the formation process of the organosilane monolayers and synthesis of silanization reaction in hydrocarbon solvent, such as toluene, bicyclohexyl, hexadecane, etc. [11]. In some cases of the liquid-phase modification, microdefects often exist at the modified surface because the SAM formation is thought to involve self-assembly of monomer or small oligomer units on the surface in a noncovalent manner to give well-ordered monolayer domains or islands on the surface surrounded by bare substrate [12–15]. Such a silane formation on silica surface shows that island formation occurs leading to a multilayer [16]. Hence, in order to achieve complete modification, precise control of the modification procedure is required. On the other hand, more recently, the monolayer modification process by quite a simple method of using a gas-phase silanization reaction, that is a CVD method, is proposed by Sugimura et.al. for application on ultrahigh resolution patterning resists and patterned monolayer templates [17–23]. This method has proved to have the capability to form homogenous, defect-free monolayer coating onto the surfaces [17–20], which is believed to be suitable for our objective.

Si(100) wafers covered with thermally grown silicon oxide were used for the work. The silicon oxide film was formed at 950°C at N_2 atmosphere. Three types of organosilanes, that is, octadecyltrimethoxysilane (ODMS), (heptadeca-fluoro-1,1,2,2-tetrahydro-decyl)trimethoxysilane (FAS), and 3-aminopropyltriethoxysilane (APS), were used as precursors. The wafers were placed together with an organosilane (ODMS or FAS) bial, and then heated at a constant temperature of 110°C. In the case of APS, the wafers were immersed in toluene solvent including 1 vol% APS liquid at 60°C as the formation of the APS monolayer was found to proceed easily in the liquid phase, rather than in the gas phase. It has been reported that complete monolayers are used for these modification procedures. The thickness of the organosilane monolayers formed was estimated to be 20 Å (ODMS), 13 Å (FAS), and 6 Å (APS), respectively. Water-contact angles of these monolayer-covered SiO_2/Si substrates were 105° (ODMS), 120° (FAS), 60° (APS), respectively. These values correspond to previous reports [17–19, 24, 25]. Figure 10.3 shows contact mode AFM images of the modified surfaces measured under a near-contact condition at low tip-pressure. The RMS and R_a values for each modified surface are indicated to be similar to those of the bare silicon oxide surface. Therefore, it is suggested that the modified surfaces are flat and uniformly formed at the monolayer level.

Chemical properties and coverage of the modified surface were characterized by XPS. Figure 10.4 shows the carbon (1s) narrow spectra of the modified surfaces. The coverage of modified surface was calculated by using the integrated peak areas of the carbon (1s) and silicon (2p) XPS narrow scans. Table 10.1 lists the ratio of organic adsorbates per all reaction sites of ideal quartz surface, and the

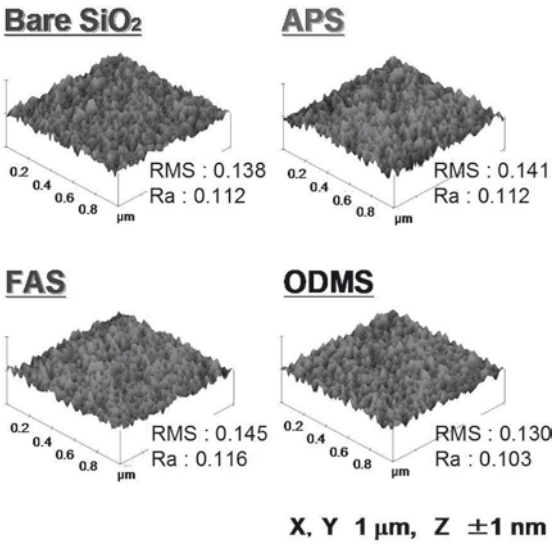

Fig. 10.3 Contact mode AFM images of organosilane modified SiO_2 surfaces

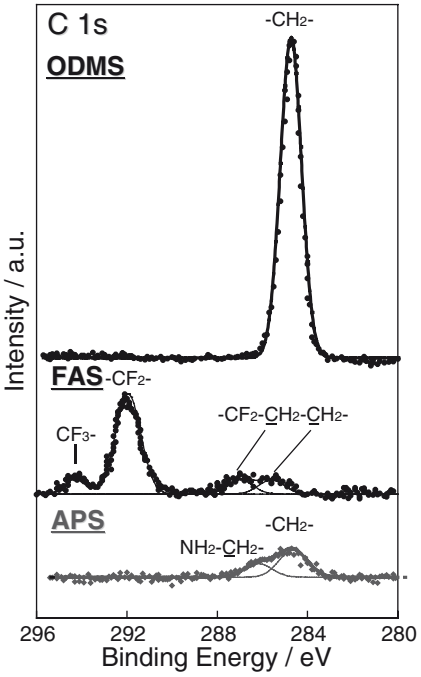

Fig. 10.4 X-ray photoelectron spectra in the C1s region of organosilane modified SiO_2 surface

Table 10.1 Coverage for each monolayer and molecular length of each moiety

	C/Si	Adsorbate areal density/SiO_2 areal density	Adsorbate areal density/maximum areal density	Molecular length/Å	
				Experimental	Calculation
ODMS	1.10	0.85	1.02	26.0	25.5
FAS	0.39	0.58	1.02	15.9	15.6
APS	0.22	0.81	1.01	6.8	6.7

areal density of the adsorbate to maximum areal density [5, 26, 27]. The maximum areal densities were adapted to the value of the cross-sectional area of each molecule, which are 18.0 $Å^2$ (ODMS), 27.5 $Å^2$ (FAS), and 20.0 $Å^2$, respectively. The areal density of ideal quartz surface is $(15.7\ Å^2)^{-1}$. The areal density of the adsorbate to the maximum areal density became the effective coverage. The areal density of each modified surface indicates nearly 1.0. Moreover, we estimated the molecular length of each moiety from the integrated peak areas of the carbon and silicon. These experimental data show expected values compared with the calculated ones (Table 10.1). Based on these XPS characterizations, it is considered that each modified surface is closely packed and is composed of a single moiety species. In addition, as described above, the modified surfaces were indicated to be flat and homogeneous from the AFM investigation. Therefore, each modified surface was expected to be formed as a monolayer.

10.1.4 Device Fabrication

A basic design of the organic monolayer-modified SiO_2 gate FET device is shown in Fig. 10.2. We selected a SiO_2 as a material for gate and protective layers on source-drain electrodes, in order to form the SAMs onto the device surface. As for the protective and gate layers, high-density, quartz-like SiO_2 such as a thermally grown SiO_2 is desired for accomplishing an ideal molecular modification (perfect coverage), and for preventing a leakage and drift during the device operation in aqueous solution. A SiO_2 as the protective layer is often formed by CVD; however, the CVD–SiO_2 layer generally shows lower density than the thermally grown one. Hence, the improvement of the property of CVD–SiO_2 layer is a critical issue for fabricating the organic monolayer-modified FET with high chemical durability. Thus, we preliminarily examined various treatments to improve the structural property of the CVD layer. In this experiment, the layer was formed by a PECVD with tetraethoxysilane (TEOS)/O_2 gas at 400°C. The property of the layer was evaluated from the value of an ellipsometric refractive index and of the etching rate with 1.0 wt% aqueous HF solution. Each value was listed in Table 10.2. When these values of the CVD–SiO_2 were compared to that of a thermally grown SiO_2 formed by dry oxidation at 950°C, the CVD layer showed a low refractive index and a high etching rate. A decrease in the refractive index and an increase in the etching rate are brought about by the lowering of the film density. It is thought that the CVD

Table 10.2 Properties of the thermally grown and the CVD SiO_2 layers

	Refractive index	Etching rate with 1.0 wt% HF (Å/min)
Thermally grown SiO_2	1.462	60
CVD–SiO_2 (as deposited)	1.449	368
CVD–SiO_2 (after 800°C annealing)	1.460	65

layer formed under the above condition is porous. Then, we carried out a postannealing process for the structural improvement of the CVD layer. By annealing the CVD layer in an O_2 atmosphere at over 800°C, the layer shows stable properties compared with the thermally grown one, as shown in Table 10.2. From these results, we decided to employ the postannealing process for the CVD–SiO_2 layers to stabilize its properties.

Figure 10.5 illustrates the process step for fabrication of the monolayer-modified FETs. Field and gate SiO_2 layer was formed on p-type Si(100) surface. P^+ ions were implanted for forming source and drain channels. In order to fabricate the device with a high temperature process, we selected a $TiSi_2$ as a contact metal. Ti and Pt were sequentially evaporated to source and drain regions, and the substrate was annealed at 800°C to form the $TiSi_2$ electrodes (Fig. 10.5a). Then, the whole surface was covered with the SiO_2 using TEOS–PECVD. After the postannealing for the structural improvement of the CVD–SiO_2 layer described above (Fig. 10.5b), the CVD–SiO_2 layer on the thermally grown gate oxide was positioned selectively removed by a reactive ion etching. Modification of organosilane molecules and their patterning process were carried out (Fig. 10.5c). The FAS and APS were formed by the method described. A position-selective formation of monolayers, having different functional groups, onto the substrate was performed by using photo-lithography process. The FAS monolayer modified substrate was covered with conventional photo-resist, and then patterning was carried out with an ultraviolet (UV) lamp.

This patterned substrate was exposed to O_2 plasma for removal of the monolayer (Fig. 10.5d). The resist pattern was used as the mask for plasma ashing. After this process, photo-resist was removed and the amino silane monolayer was formed on the exposed clean oxide layer (Fig. 10.5e).

10.1.5 Device Characteristics

The fabricated FET devices that are modified with organosilane monolayers are shown in Fig. 10.6. The gate length and width of the devices are 10 μm and 1 mm, respectively. The separation between contacts and SiO_2 gate is 10 μm.

Figure 10.7 shows I_{ds}–V_{ds} curves of the amino-monolayer modified FET in pH 6.86 buffer solution. The characteristics indicated typical FET response, which were stable during a long-time immersion of upto 24 h. Also, the I_{ds}–V_{ds} profile of the

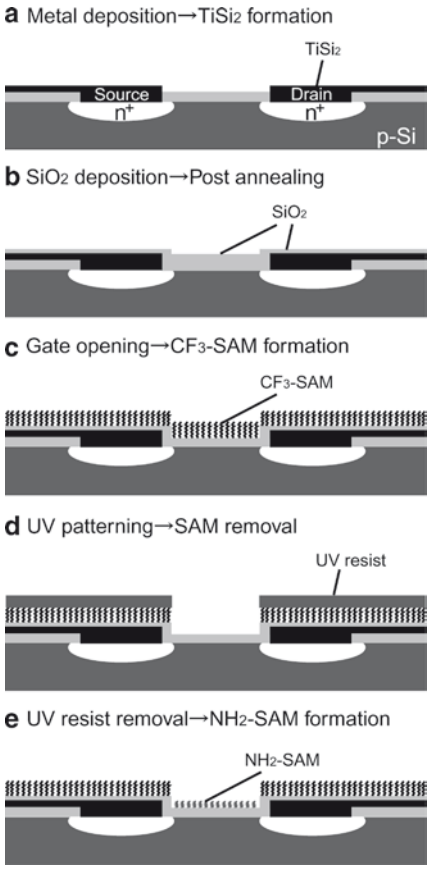

Fig. 10.5 Process steps for fabrication of the monolayer modified FETs

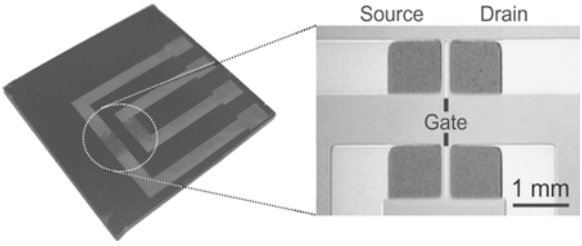

Fig. 10.6 Photograph and optical microscopy image of the fabricated monolayer modified FETs

device was reproducible even if the monolayer removing by O_2 plasma ashing and the modification process involving the treatment of strong acid were repeated many times using the process described above. Therefore, this device was quite stable in aqueous solution, and had a high chemical durability. The I_{ds}–V_g curves of the amino-modified FET in various pH solutions are shown in Fig. 10.8a. The V_{th} shifts depending on the

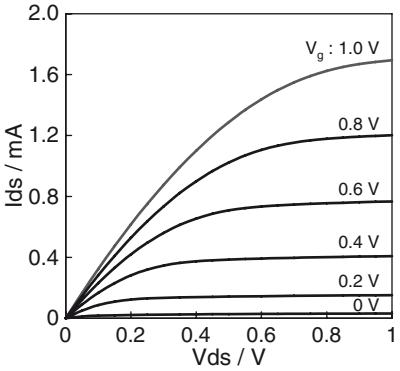

Fig. 10.7 I_{ds}–V_{ds} characteristics of the amino-monolayer modified FET

change in the pH value in the solution. As seen in Fig. 10.8b, the V_g linearly changes depending on pH at the sensitivity of 58 mV/pH. This pH sensitivity is quite similar to that of an ISFET such as the Si_3N_4 gate FET [1, 4, 28], which shows a good Nernstian response. On the contrary, in the case of the FAS monolayer modified FET, the potential remains constant, regardless of the pH values in the solution.

The shift of the V_{th} depends on the changes of surface potential at liquid/monolayer interface. For the APS-modified surface, both unreacted Si–OH and O–Si–$(CH_2)_3$–NH_2 sites exist at the surface. Thus, it is thought that the APS-modified FET shows pH response in solution. On the other hand, the FAS-modified surface is a well-ordered and highly hydrophobic surface because the perfluoro alkyl moiety is long-chain and hydrophobic. Such the surface is expected to block the solution, and can inhibit the reaction of the unreacted Si–OH sites with ionic species in the solution, resulting in no pH response in the solution. From these investigations, the pH response of these surfaces is indicated to significantly affect by a variation in functional group. The APS-modified FET has the capability to be used as an ISFET, and the FAS-modified FET is applicable to a reference electrode. It is expected that the fabrication of the monolayer-modified FETs is effective for fabrication of on-chip ion-sensing devices including reference electrodes.

10.2 FET Biosensor

10.2.1 Introduction

Biosensing systems, such as enzyme, immuno sensors and DNA micro arrays, are widely used in the field of medical care and medicine manufacturing [29–31]. In particular, recent progress in genome engineering requires high performance integrated micromulti-biosensing system, which can be utilized for recognition of individual

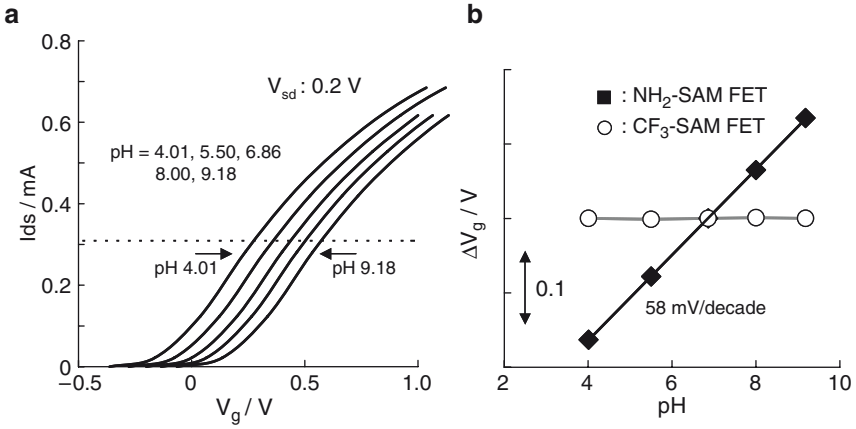

Fig. 10.8 (**a**) I_{ds}–V_g characteristics of the monolayer modified devices in each pH solution. (**b**) pH-potential profiles of each monolayer modified FET

biomolecule and analysis of bioreaction at single molecular level. In the field of the advanced medical care, simple and high accuracy detection systems are essentially required for the application of a tailor-made medical diagnosis. The mainstream of the present biosensor is *fluorescent detection*. This technique has contributed to several analyses for biomolecule reaction including genome sequences. However, since typical biosensing systems based on fluorescent detection, such as DNA microarrays consist of lasers and complex optical systems, the instruments tend to become quite large-scale and expensive. Also, modification of fluorescent dye to the target biomaterials is necessary for the fluorescent detection, leading to a high-cost and complicated protocol. Therefore, new detection systems designed for simplicity and high performance are demanded for future advanced medical care.

Here, we have proposed a detection system utilizing a semiconductor device especially to FET as a sensing system that enables to achieve both simplicity and high sensitivity. Semiconductor device manufacturing technologies enable to integrate and miniaturize the device. In addition, it is easy to miniaturize and simplify the system for the device control because the system can operate by using an electrical circuit instead of an optical one. The detection using FET does not require any label materials and mediators since the surface-potential change caused by an interfacial reaction between the solution and the recognition surface can be detected by using FET as an electric signal, directly. Such a detection system by using electric signal is expected to be applicable to biosensors equipped with small size and high performance.

10.2.2 Attachment of Biomolecules onto the Recognition Region

Position-selective immobilization of biomolecules has attracted much interest in recent years for performing biological recognition and fabricating miniaturized, array-based assay devices [32–34]; for example, DNA and protein microarray chips are widely used to probe gene sequence and protein level in cells. The miniaturized feature of the device makes it possible to achieve a higher integration density of the arrays of probe molecules, thus allowing the assay to be performed at a high accuracy. The immobilization sites of biomolecules formed precisely in the micro/nano-scopic scale can be applied for conducting highly accurate biomolecular analyses, such as genotyping of single-nucleotide polymorphisms, analysis of proteins for structure and functionality, and recognition of a single molecule. The surfaces for bioanalyses are required to have an ordered, supramolecular structure that mimics cell systems. In order to form such surfaces, the application of templates for the ordered arrangement of the molecules is effective. Surfaces modified with SAMs are suitable for this purpose, and the immobilization of biomolecules on bare gold and SiO_2 surfaces has been reported [11, 35–37]. It is generally recognized that the modified surfaces are preferable to immobilization of specific molecular species. For patterning of the molecules, methods including microcontact printing, ink-jet delivery, dip-pen nano-lithography, and nano-manipulation using scanning probe microscopy have been proposed. On the other hand, we investigated the process for fabricating molecular templates at micro and nano scales using UV and electron-beam lithography [5, 38, 39]. These processes aid the controlled formation of SAMs having various functional groups under self-assembling conditions, with a precise position selectivity to form active and passive sites for immobilization of biomolecules.

Figures 10.9b and c show representative fluorescence microscope images of the surface patterned with organosilane monolayers after immobilization of the fluorescence-labeled oligonucleotides. In these images, bright dot-patterns indicating the existence of oligonucleotides are clearly seen. These regions correspond to the APS-patterned regions formed on the surface. In contrast, when patterned surfaces without modification by aminosilane were used, no bright regions were observed in fluorescence microscope images, indicating thereby that the oligonucleotides were *not* immobilized on the surface. These results show that the oligonucleotides were position-selectively immobilized only on APS-modified sites formed on the patterned-monolayer surface at micro and nanometer scales, and ODMS-modified surfaces acted as a layer for preventing the non-specific attachment of oligonucleotides. A similar controlled immobilization was also achieved when a template surface cross-linked with biotin molecules was used. Moreover, the specific reaction between biotin and streptavidin was detected by using the monolayer template surface (Fig. 10.9d, e). These results suggest the usefulness of patterned monolayer templates for *immobilizing* biomolecules and for *promoting* interaction between biomolecules with a high selectivity.

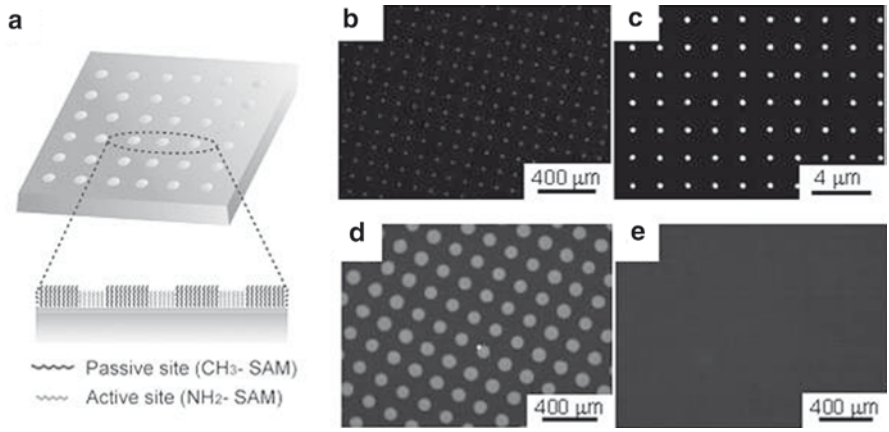

Fig. 10.9 (**a**) Schematic illustration of the surface patterned with different monolayers. (**b**, **c**) Representative fluorescent microscope images of the APS/ODS patterned surface covalently immobilized with oligonucleotide (**d**, **e**) fluorescence images of the patterned surface modified (**d**) with and (**e**) without biotin after the reaction

10.2.3 FET Biosensor Using Enzymatic Reaction

As one of the applications of the monolayer-modified FETs to biosensing, we have performed urea detection by using an enzymatic reaction. An enzymatic hydrolysis reaction of urea by urease, which shifts the pH toward higher values depending on the quantity of urea, was focused upon [40].

The quantity of urea was estimated from the shift of the gate voltage of an enzyme-immobilized APS FET. Note that the gate voltage of the APS-modified FET shifts depending on the change of pH at the interface between a solution and the gate surface. Figure 10.10a shows I_{ds}–V_g curves of the enzyme-modified FET in the solutions containing different urea concentrations. The I_{ds}–V_g profile shifts to the positive direction (high pH direction) according to the concentration of urea in the solution. The calibration curve is shown in Fig. 10.10b. The gate voltage linearly changes toward urea concentration with a high sensitivity of 64 mV/decade in the range of 10^{-9}–10^{-6} M. However, calibration curve shows the tendency to saturate in the range of over 10^{-6} M. Such a difference in the response is thought to be related to the amount of enzyme immobilized onto the APS surface. Since the APS monolayer surface is quite flat, the amount of enzyme immobilized onto the surface could be relatively low. Therefore, in the case of the urea concentration of over 10^{-6} M, it seems that an ureolysis ability of the enzyme has been exceeded, resulting in the decrease in the voltage shift. From the result, it is indicated that the FET device with enzyme immobilized onto the APS monolayer has a high capability for the detection of trace concentration of urea.

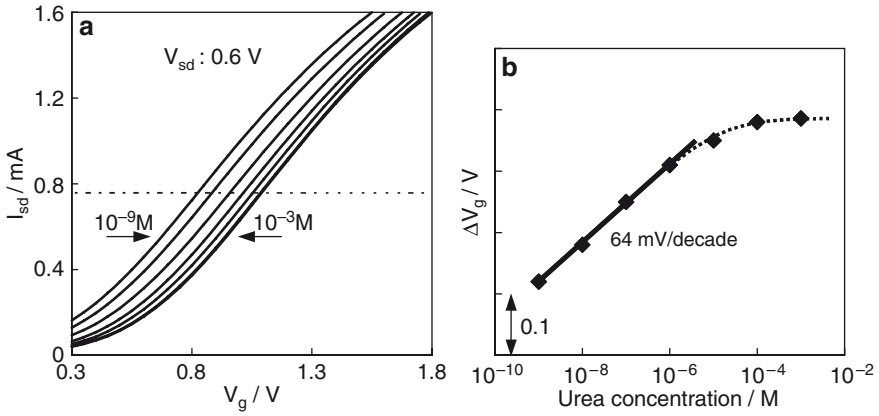

Fig. 10.10 (**a**) I_{ds}–V_g curves of enzyme immobilized FET in the solution containing different concentration of urea. (**b**) Calibration curve of the enzyme immobilized device for urea detection

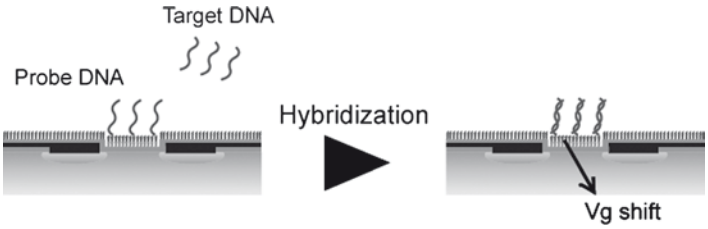

Fig. 10.11 Scheme of hybridization reaction between the immobilized DNA (probe DNA) and Target DNA

10.2.4 DNA Sensor Using FET

The detection of hybridization reaction of DNA was studied in our active under-investigation research.(Fig. 10.11). If DNA is attached to the surface, the surface potential shifts in the negative direction since DNAs have a negative charge originated from deprotonated phosphate esters in aqueous solution. Moreover by hybridizing DNA at the surface, the potential shifts to more negative. Based on the property of DNA itself, detection of DNA-SNPs was carried out. The V_{fg} of the probe DNA-immobilized FET shifted due to the negative charge while DNA, on the surface, hybridized with complementary DNA. The results revealed that the V_g

shifted by 53 mV in the case of using 20-mer DNA. It was also noted that no shift was observed when using noncomplementary DNA. In addition, the voltage shifts depending on the number of mismatches observed in DNA. Therefore, the DNA-immobilized FET is expected to have a high potential for the detection of SNPs with high sensitivity and selectivity.

10.3 Conclusion

The FET device has a high potential for the detection of ions and biomaterials. As described in some examples, the application of the FET as a sensor is expected to be useful for the next generation high-performance, on-chip sensing system. In addition, since the FET sensor enables the miniaturization of the sensor chip itself, it is especially expected to apply the advanced medical care and tailor-made medical diagnosis. Moreover, the combination between nanotechnology and biotechnology will accelerate the fusion of various industries such as the semiconductor industry and bioventures.

References

1. Matsuo T, Esashi M (1981) Methods of ISFET fabrication. Sens Actuators 1:77–96
2. Bergveld P (1972) Development, operation, and application of the ion-sensitive field-effect transistor as a tool for electrophysiology. IEEE Trans Biomed Eng BME-19:342–351
3. Matsuo T, Wise KD (1974) An integrated field-effect electrode for biopotential recording. IEEE Trans Biomed Eng BME-21:485–487
4. Bousse L, Mostarshed S, Van der Schoot B, de Rooij NF (1994) Comparison of the hysteresis of Ta_2O_5 and Si_3N_4 pH-sensing insulators. Sens Actuators B 17:157–164
5. Niwa D, Yamada Y, Homma T, Osaka T (2004) Formation of molecular templates for fabricating on-chip biosensing devices. J Phys Chem B 108:3240–3245
6. Niwa D, Homma T, Osaka T (2004) Fabrication of organic monolayer modified ion-sensitive field effect transistors with high chemical durability. Jpn J Appl Phys 43:L105–L107
7. Niwa D, Omichi K, Motohashi N, Homma T, Osaka T (2006) Organosilane self-assembled monolayer-modified field effect transistors for on-chip ion and biomolecule sensing. Sens Actuator B 108:721–726
8. Kuroiwa S, Wang J, Satake D, Nomura S, Osaka T (2009) Effect of surface morphology of reference field effect transistor modified by octadecyltrimethoxysilane on ionic responses. J Electrochem Soc 156:J67–J72
9. Wang J, Ito K, Nakanishi T, Kuroiwa S, Osaka T (2009) Tb^{3+}-enhanced potentiometric detection of single nucleotide polymorphism by field effect transistors. Chem Lett 38:376–377
10. Ulman A (1991) An introduction to ultra thin organic films from langmuir-blodgett to self-asembly. Academic, San Diego, CA
11. Wasserman SR, Tao Y-T, Whitesides GM (1989) Structure and reactivity of alkylsiloxane monolayers formed by reaction of alkyltrichlorosilanes on silicon substrates. Langmuir 5:1074–1087

12. Schwartz DK (2001) Mechanisms and kinetics of self-assembled monolayer formation. Annu Rev Phys Chem 52:107–137
13. Doudevski I, Hayes WA, Schwartz DK (1998) Submonolayer island nucleation and growth kinetics during self-assembled monolayer formation. Phys Rev Lett 81:4927–4930
14. Leitner T, Friedbacher G, Vallant T, Brunner H, Mayer U, Hoffmann H (2000) Investigations of the growth of self-assembled octadecylsiloxane monolayers with atomic force microscopy. Mikrochim Acta 133:331–336
15. Iimura K, Nakajima Y, Kato T (2000) A study on structures and formation mechanisms of self-assembled monolayers of n-alkyltrichlorosilanes using infrared spectroscopy and atomic force microscopy. Thin Solid Films 379:230–239
16. Wang Y, Lieberman M (2003) Growth of ultrasmooth octadecyltrichlorosilane self-assembled monolayers on SiO_2. Langmuir 19:1159–1167
17. Sugimura H, Ushiyama K, Hozumi A, Takai O (2000) Micropatterning of alkyl- and fluoroalkylsilane self-assembled monolayers using vacuum ultraviolet light. Langmuir 16:885–888
18. Hozumi A, Ushiyama K, Sugimura H, Takai O (1999) Fluoroalkylsilane monolayers formed by chemical vapor surface modification on hydroxylated oxide surfaces. Langmuir 15:7600–7604
19. Sugimura H, Nakagiri N (1997) Organosilane monolayer resists for scanning probe lithography. J Photopolym Sci Technol 10:661–666
20. Sugimura H, Nakagiri N (1996) Scanning probe anodization: nanolithography using thin films of anodically oxidizable materials as resists. J Vac Sci Technol A 14:1223–1223
21. Hozumi A, Sugimura H, Yokogawa Y, Kameyama T, Takai O (2001) ζ-potentials of planar silicon plates covered with alkyl- and fluoroalkylsilane self-assembled monolayers. Colloid Surf A 182:257–261
22. Hayashi K, Saito N, Sugimura H, Takai O, Nakagiri N (2002) Regulation of the surface potential of silicon substrates in micrometer scale with organosilane self-assembled monolayers. Langmuir 18:7469–7472
23. Sugimura H, Hanji T, Hayashi K, Takai O (2002) Surface potential nanopatterning combining alkyl and fluoroalkylsilane self-assembled monolayers fabricated via scanning probe lithography. Adv Mater 14:524–526
24. Siqueira PDF, Wenz G, Schunk P, Schimmel T (1999) An improved method for the assembly of amino-terminated monolayers on SiO_2 and the vapor deposition of gold layers. Langmuir 15:4520–4523
25. DePalma V, Tillman N (1989) Friction and wear of self-assembled trichlorosilane monolayer films on silicon. Langmuir 5:868–872
26. Barrelet CJ, Robinson DB, Cheng J, Hunt TP, Quate CF, Chidsey CED (2001) Surface characterization and electrochemical properties of alkyl, fluorinated alkyl, and alkoxy monolayers on silicon. Langmuir 17:3460–3465
27. Cicero RL, Linford MR, Chidsey CED (2000) Photoreactivity of unsaturated compounds with hydrogen-terminated silicon(111). Langmuir 16:5688–5695
28. Niu MN, Ding XF, Tong QY (1996) Effect of two types of surface sites on the characteristics of Si_3N_4-gate pH-ISFETs. Sens Actuators B 37:13–17
29. Birge RR (ed) (1994) Molecular electronics and bioelectronics. Am Chem Soc, Washington, DC
30. Bard AJ (1994) Integrated chemical systems. Wiley, New York
31. Spochiger-Kuller UE (1998) Chemical sensors and biosensors for medical and biological applications. Wiley, Washington
32. Schena M, Shalon D, Davis RW, Brown PO (1995) Quantitative monitoring of gene expression patterns with a complementary DNA microarray. Science 270:467–470
33. MacBeath G, Schreiber SL (2000) Printing proteins as microarrays for high-throughput function determination. Science 289:1760–1763
34. Wilson DS, Nock S (2003) Recent developments in protein microarray technology. Angew Chem Int Ed 42:494–500

35. Frutos AG, Smith LM, Corn RM (1998) Enzymatic ligation reactions of DNA "words" on surfaces for DNA computing. J Am Chem Soc 120:10277–10282
36. Lamture JB, Beattie KL, Burke BE, Eggers MD, Ehrlich DJ, Fowler R, Hollis MA, Kosicki BB, Reich RK, Smith SR, Varma RS, Hogen ME (1994) Direct detection of nucleic acid hybridization on the surface of a charge coupled device. Nucleic Acids Res 22:2121–2125
37. Souteyrand E, Cloarec JP, Martin JR, Wilson C, Lawrence I, Mikkelsen S, Lawrence MF (1997) Direct detection of the hybridization of synthetic homo-oligomer DNA sequences by field effect. J Phys Chem B 101:2980–2985
38. Niwa D, Omichi K, Motohashi N, Homma T, Osaka T (2004) Formation of micro and nano-scale patterns of monolayer templates for position selective immobilization of oligonucleotide using ultraviolet and electron beam lithography. Chem Lett 33:176–177
39. Osaka T, Matsunaga T, Nakanishi T, Arakaki A, Niwa D, Iida H (2006) Synthesis of magnetic nanoparticles and their application to bioassays. Anal Bioanal Chem 384:593–600
40. Osaka T, Komaba S, Seyama M, Tanabe K (1996) High-sensitivity urea-sensor based on the composite film of electroinactive polypyrrole with polyion complex. Sens Actuators B 36:463–469